THE DEVELOPMENT OF A FULL FIELD THREE-DIMENSIONAL MICROSCALE FLOW MEASUREMENT TECHNIQUE FOR APPLICATION TO NEAR CONTACT LINE FLOWS

Qun He and Kevin Hallinan
University of Dayton
Department of Mechanical and Aerospace Engineering
Dayton, Ohio 45460-0210

BACKGROUND

The goal of this paper is to present details of the development of a new three-dimensional velocity field measurement technique which can be used to provide more insight into the dynamics of thin evaporating liquid films (not limited to just low heat inputs for the heat transfer) and which also could prove useful for the study of spreading and wetting phenomena and other microscale flows.

Traditional velocity measurement techniques, such as hot-wire and laser Doppler anemometry (LDA) and standard Particle Image Velocimetry (PIV), are unable to provide velocity information in such thin films. The Forward Scattering Particle Image Velocimetry (FSPIV) technique developed by Ovryn and Hovenac (1993) offers the most promise. In this scheme, shown schematically in Figure 1, a partially coherent light beam back illuminates a mono-disperse suspension of spherical particles seeded in a fluid which ideally follow the fluid pathlines. A video microscopy system is used to view and record the forward scattered and transmitted light. Ovryn et al. has demonstrated that the light scattering produces a unique diffraction like image of the particle in the image plane for each de-focus position of the particles. This characteristic was exploited to determine the particle de-focus distance and the paraxial velocity if the time between the video frames is known. Simultaneously the transverse velocity (normal to the optical axis) was calculated by finding the particle centroid trajectories over time.

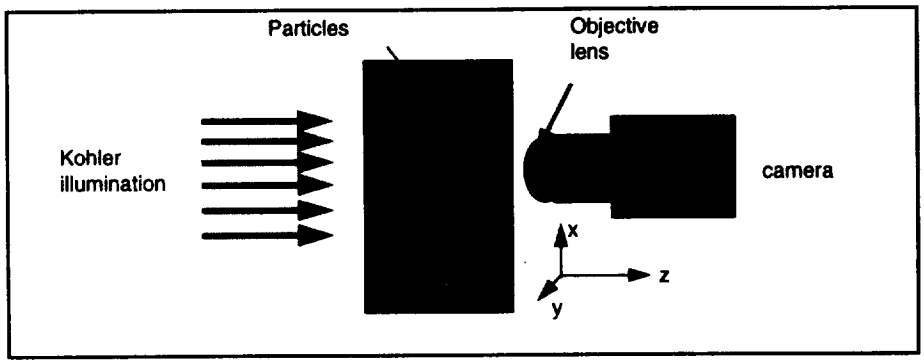

Figure 1. - Schematic of FSPIV.

Figure 2(a)-(c) show some examples of the scattered/transmitted light patterns of a spherical PMMA particle with a diameter of 0.325 micron in liquid methanol. Figure 2(d)-(e) are the intensity profiles of the diffraction images along the rows shown in the images. Apparent from these figures is that the diffraction patterns are different for equal and opposite paraxial defocus distance ("+" means closer to the objective, "-" means further away from the objective). The reason for this asymmetry has been shown in yet unpublished work by Khaydarov and Ovryn to be due to the transmission of light through the particles.

To obtain particle velocities, after acquiring the active particle images and ignoring any agglomerated particle images, the centroids of the scattered light images associated with each of the particles are first identified

in each frame[1]. The next step is to track individual particle centroids from frame to frame. The most widely used method is a two frame cross-correlation approach. Determining the particle centroids displacement over time provides the transverse velocity[2]. The axial velocity can be determined by identifying the rate of change of the de-focus distance of each particle.

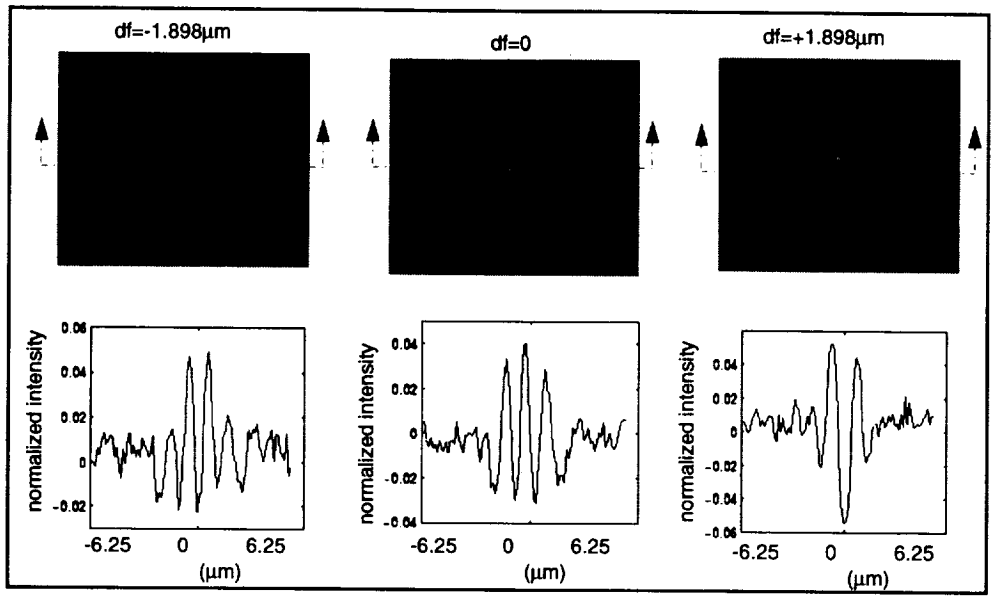

Figure 2. - Diffraction pattern and cross sectional intensity profile.

Establishing a relationship between the defocus of the particles and their scattering pattern is the most crucial aspect of this technique. A theoretical determination of this relationship is possible using Lorenz-Mie scattering theory. However, using theoretical predictions as a standard to compare to experimental measurements presumes an a priori knowledge of the optical aberrations of the experimental imaging and illumination systems. Alternatively, an experimental standard of 'calibration' images can be created and used. These 'calibration' images require that the image of near focus particles be obtained at known and different defocus distances. Then, the de-focus distance of an active can be determined by comparison to a look-up-table (LUT) of calibration images using a correlation based pattern recognition technique. The active particle de-focus position is identified with the de-focus of the calibration image which produces the best correlation.

The correlation involves integrating over space the product of the active particle image intensity, f(x, y) and the intensity of each image in the bank of calibration images, g(x,y). Before correlating, however, the calibration and input images must first be normalized. This first requires the average intensity of the entire image to be determined as:

$$f_{average} = \frac{1}{M * N} \sum_{i=1}^{M} \sum_{j=1}^{N} f(i,j)$$

where M and N are the total number of pixels in the image in x and y directions. The analogous discrete normalized pixel intensity is defined as:

$$f_{normalization}(i,j) = \left(f(i,j) - f_{average}\right) \cdot \left(\sum_{i} \sum_{j} (f(i,j) - f_{average})^2 \right)^{-1/2}.$$

[1]The centroid is easily found by identifying the center of the intensity profile.

[2]One of the limitations associated with cross-correlation particle tracking techniques for traditional PIV (i.e., the production of noise if the particles move out of the sampling region through three-dimensional motions) is not present for FSPIV.

The numerical approach for achieving the correlation is via the Fourier transform. The correlation process has a frequency space realization that involves Fourier transforming both signals and multiplying them. The correlation function is the inverse Fourier transform of this product. The mathematical representation of this process is shown below:

$$f * g = F^{-1} (F G)$$

where F and G are the Fourier transforms of f and g.

Figure 3 demonstrates the correlation pattern recognition procedure. In this figure, the active input image intensity and the bank of calibration images are shown. Each column in the bank of calibration images represents the normalized intensity profile of a particle image of known defocus. The input intensity plot is the normalized intensity of an image with unknown defocus. The correlator box shown represents the computer algorithm which makes the comparison of the unknown image to each of the calibration images. For the input image shown, the resulting correlation plot shows that the peak correlation is achieved at a defocus of -9 μm. Therefore, the input image is identified to be at a defocus of -9 μm relative to the focal plane of the imaging system, equal to the true defocus position of the active image for this example.

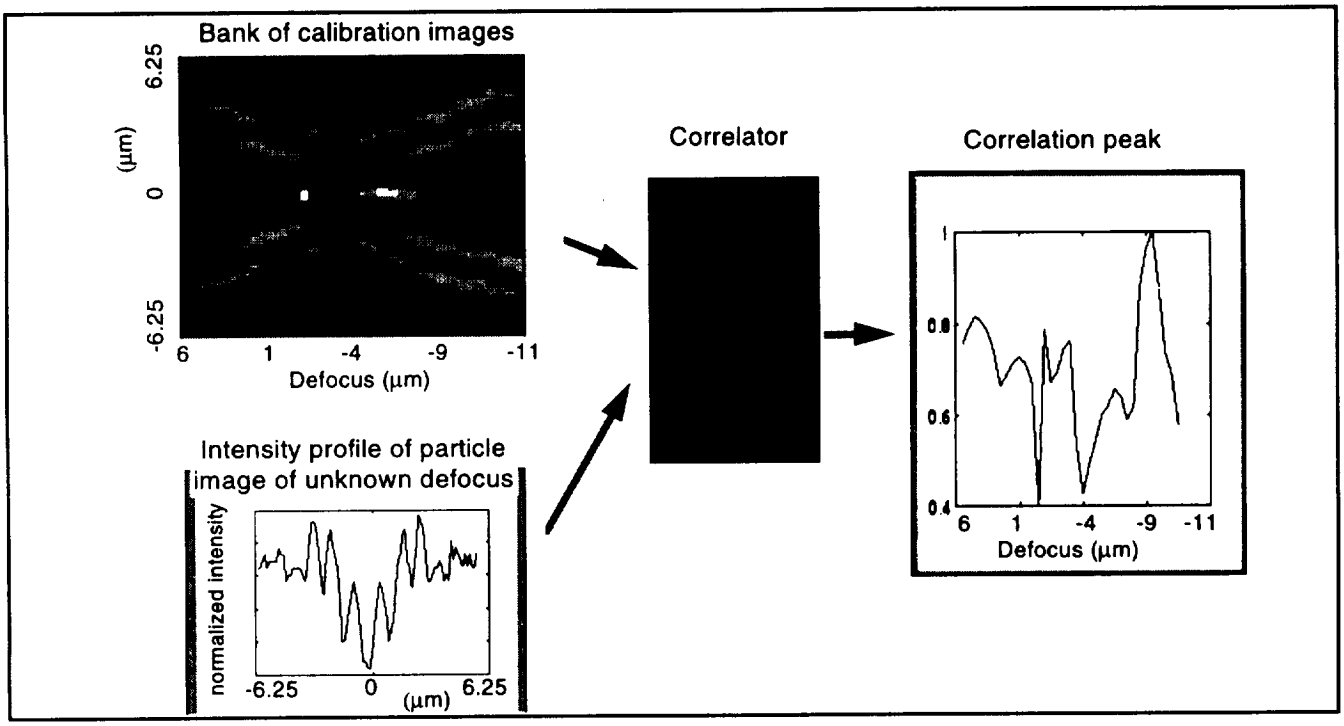

Figure 3. - Pattern recognition of diffraction images

EXPERIMENTS

It has been a challenge to configure the hardware needed to implement this technique to measure fluid velocity in the near contact line region because of the small lengthscales associated with the region of interest (300 microns in length and up to 100 microns in film thickness). The small dimensions forced the use of micron or sub-micron size particles to minimize the disturbance of the particles to the flow. This requirement dictated the use of both a high Numerical Aperture imaging lens and a highly coherent light source in order to collect the scattered light around the particles. A long working distance imaging lens was also required to compensate for the thickness of the optical window separating the seeded liquid from the imaging lens. Alignment of the light source with the

optical axis of the objective lens was found to be extremely critical for producing repeatable results. Further, the development of a bank of calibration images required a very fine stage translation and accurate stage displacement micrometer since these affect the accuracy of both the determination of the particle position and paraxial velocity. Finally, the sampling time was required to be small enough to effectively freeze the particles in each frame to eliminate blurring.

Figure 4 shows a schematic of the final hardware setup for the three dimensional full field PIV technique which has been configured. A Labophot-2A microscope by Nikon with a built-in Kohler illumination system is used to view particles in a test cell mounted on the microscope stage. The light was filtered to minimize infrared heating of the liquid within the test cell. Experimental details are presented in the figure.

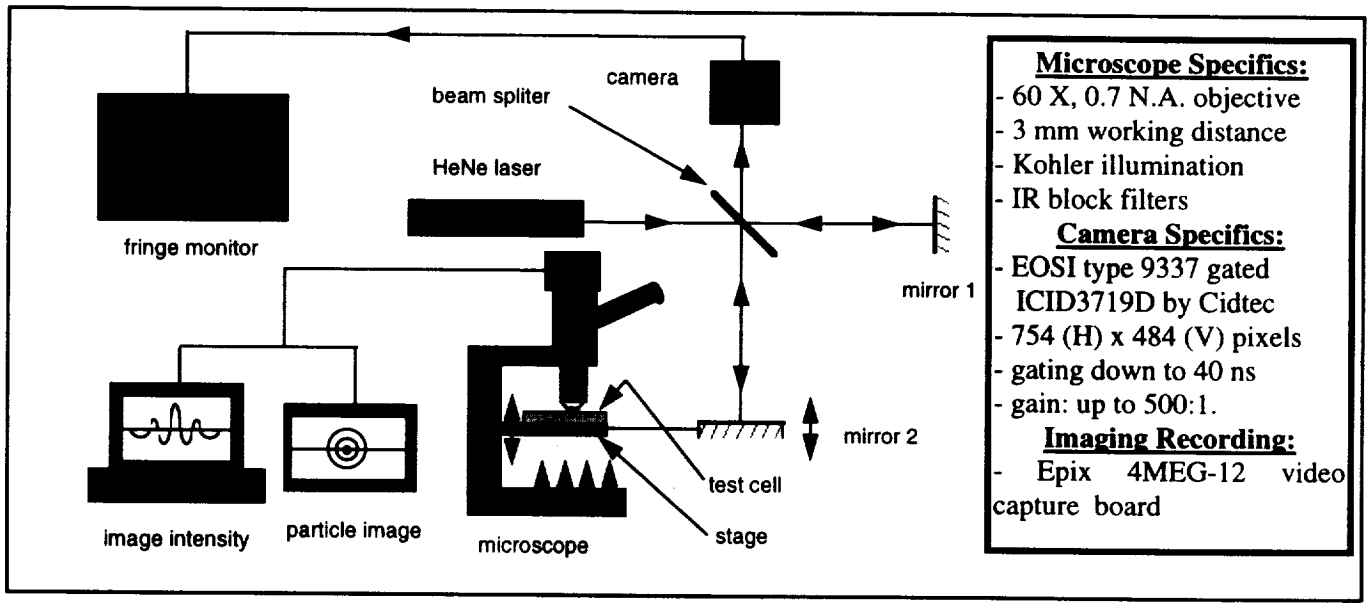

Figure 4. - Experimental setup.

The 80 mm x 80 mm x 10 mm deep test cell shown in Figure 5 is a rectangular and transparent enclosure partially filled with particle seeded liquid methanol (HPLC grade, 99.9% pure). The particles are 3.1 microns in diameter and are PolyMethylMethAcrylate (PMMA) in make-up. The enclosure is comprised of a Teflon spacer which separates two pieces of 1 mm borosilicate glass windows. There are two ports in the test cell used to inject fluid and particles into the cell. Heat input via a resistance heater (Minco) mounted to the top of the test cell and heat removal via a cooling water heat exchanger attached to the bottom of the test cell determine the thermal state within. The heat input causes the liquid to evaporate from the near contact line region of the meniscus on the upper window. The cooling causes the vapor to condense on the bottom window. Thermocouples mounted within the cell and along the upper wall of the cell are used to identify the thermal conditions present near the contact line and within the bulk of the liquid and vapor.

The calibration images were obtained by imaging a particle fixed on the test cell wall after liquid was added. The imaging optics were then adjusted to obtain the best 'focus' of the particle. The stage was then translated both up and down by known distances to move the particle in and out of focus. The resulting particle images were recorded for these known de-focus distances. The stage translation was measured with an accuracy of ± 0.06 microns using the Michelson interferometer shown schematically in Figure 4.

To establish the viability of the three dimensional full field forward scattering particle image velocimetry technique and apply it to the velocity measurement in an evaporating extended meniscus, velocity measurement experiments were conducted on the thin film region of a meniscus formed along a heated inclined plate. Tests were conducted for variable heat input and inclination angle. Temperatures were monitored until equilibrium was established. At this point, active particle images were recorded.

RESULTS AND DISCUSSION

The initial experiments demonstrated that in the curved thin film region near the contact line, the image of the particle was found to be asymmetric such as shown in Figure 6. Figure 6(a) is the image of a particle at the flat adsorbed film region of the meniscus. Figure 6(b) is the image of a particle within the slightly curved thin film region approximately 70 microns away. Figure 6(c) is the image of a particle another 200 microns upstream. The asymmetry is due to the refraction of the incident light by the liquid-vapor interface before it interacts with the particles. When the liquid-vapor interface is not parallel with the focal plane of the imaging lens, the wave incised upon the particles is no longer planar relative to the focal plane. Also, the refraction angle of the incident wave is clearly different at different film slope. Consequently, calibration images at known film locations (i.e., for known local film slope) were generated and used to compare active images. Therefore, at discrete film slopes, a calibration Look-up-Table (LUT) similar to that shown in Figure 3 was generated.

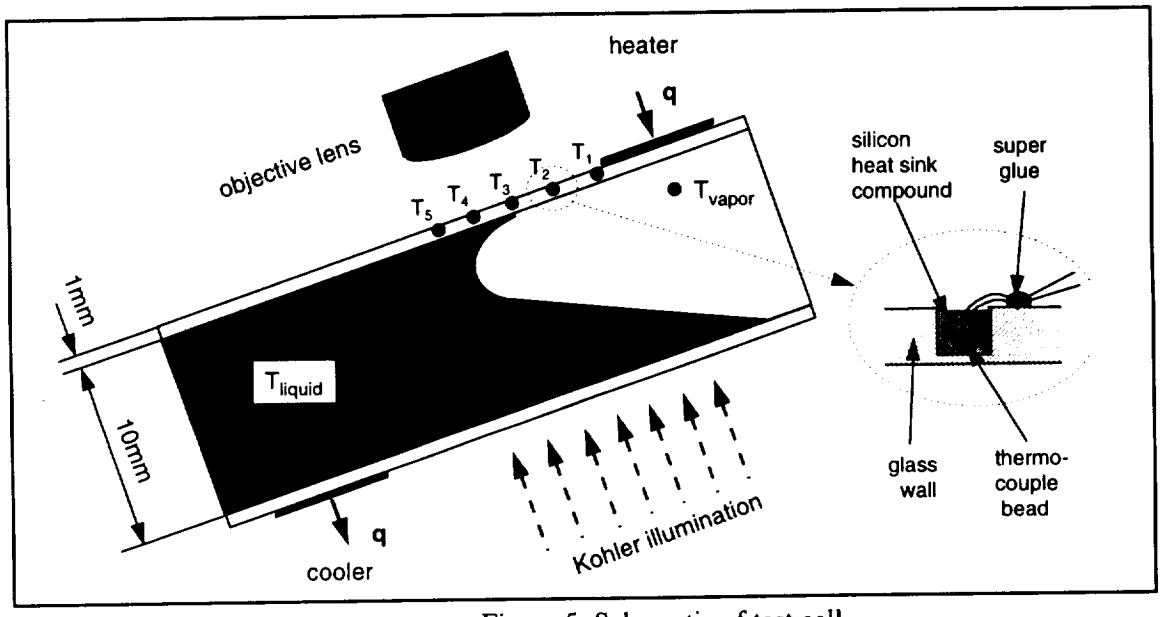

Figure 5: Schematic of test cell.

Figure 7(a) shows the trajectory of a single particle at a distance of 240 microns from the actual contact line for test conditions of 0.6 W heat input and a 4.1° inclination angle. (1/30 second interval between images). In this image, the background illumination of the image was subtracted. The centroid was computed for each particle position. From this particle trajectory, the velocity field was determined. Figure 7(b) shows the liquid through the cross-section of the liquid film. It is clear from the figure that thermocapillary stresses cause the flow to reverse near the contact line. The uncertainty of the velocity measurement is: u±9.3μm/s, v±7.5μm/s and w±15μm/s.

CONCLUSIONS

The FSPIV technique has been employed and used to measure the three-dimensional velocity field near the contact line of a curved and evaporating meniscus on a heated plate. While a significant amount of work remains to be done, its potential for application to dynamic near contact line flows has been demonstrated.

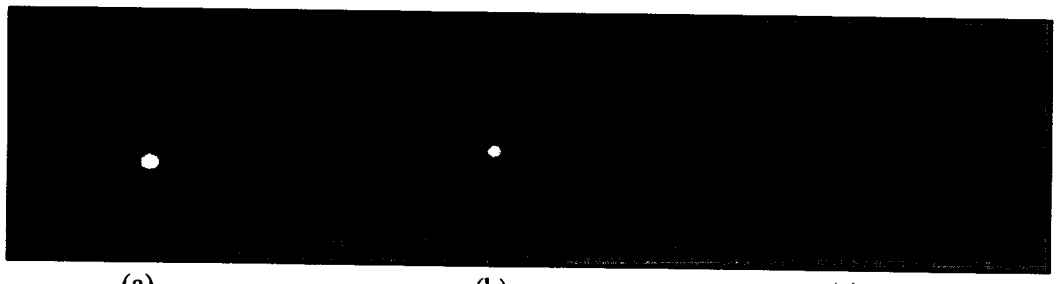

(a) (b) (c)

Figure 6. - Diffraction of particles in curved thin liquid film

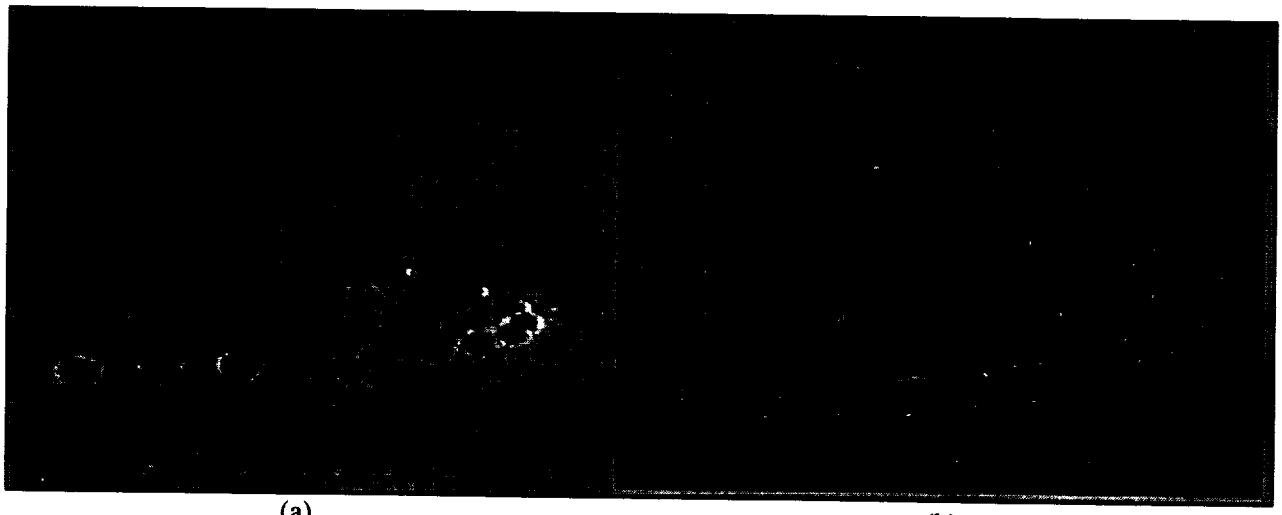

(a) (b)

Figure 7. - (a) Images of a moving particle in thin film region with inclination angle: 4.1° and heat input 0.6 watt and (b) resulting film velocity profile.

ACKNOWLEDGMENT

Thanks are due to Dr. B. Ovryn of NYMA, Inc. for his suggested use of the FSPIV technique. We would also like to acknowledge the support for this research by NASA through grant NAG3-1391.

BIBLIOGRAPHY

Ovryn, B. and Hovenac, E.A., "Coherent forward scattering particle image velocimetry: application of Poisson's spot for velocity measurements in fluids," SPIE 2005, 338-348 (1993).